

*Make file*

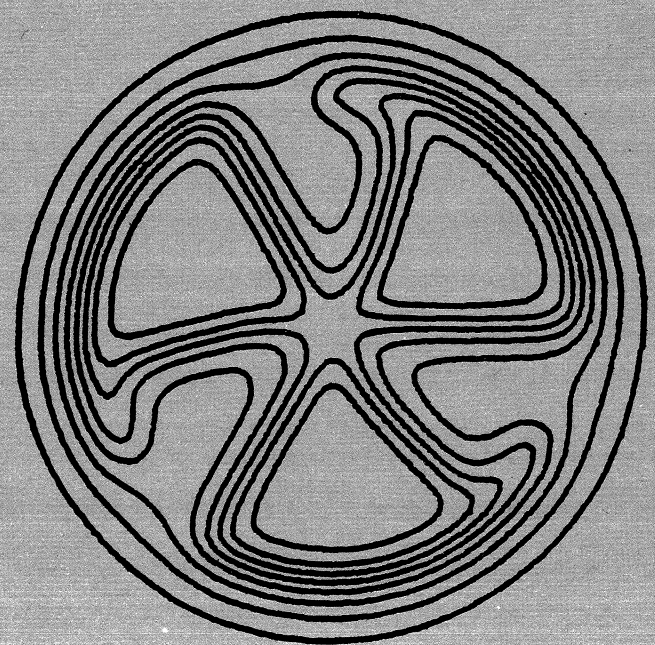
*121*

MICHIGAN STATE UNIVERSITY

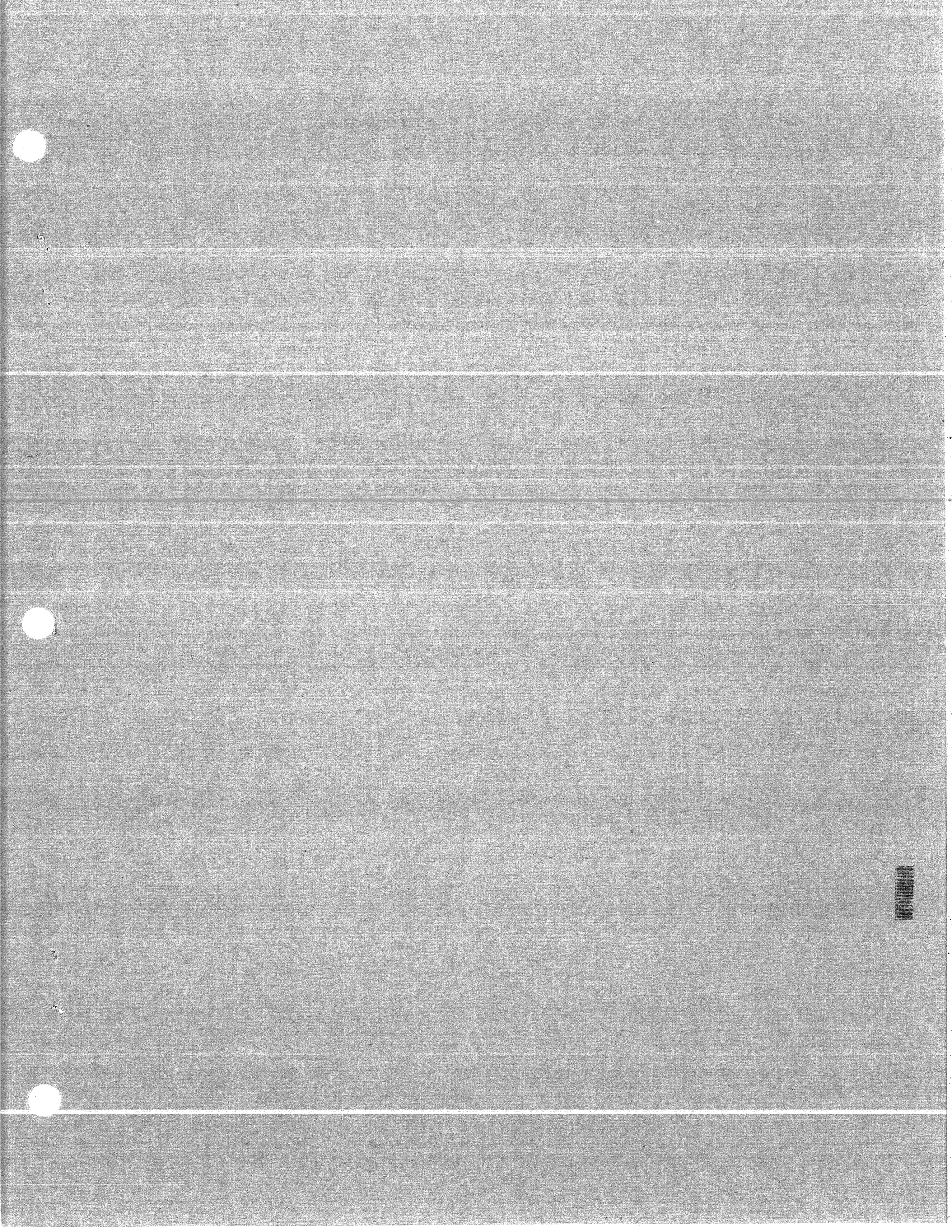
CYCLOTRON LABORATORY

A STUDY OF THE NUCLEAR CONTINUUM IN  $^{16}\text{O}$   
BY INELASTIC  $^3\text{He}$  SCATTERING

A. MOALEM, W. BENENSON, and G.M. CRAWLEY







A Study of the Nuclear Continuum in  $^{16}\text{O}$

by Inelastic  $^3\text{He}$  Scattering<sup>†</sup>

A. Moalem, W. Benenson and G. M. Crawley  
Cyclotron Laboratory and Physics Department  
Michigan State University, East Lansing, Mi. 48824

INTRODUCTION

Inelastic scattering of  $^3\text{He}$  particles shows strong excitation of the low energy region of the nuclear continuum. In heavier nuclei<sup>1</sup> ( $A > 60$ ) this manifests itself as a 3-5 Mev broad peak several Mev below the giant dipole resonance (GDR). The cross-section exhausts the E2 sum strength and this fact (along with a host of other information summarized in Ref. 1) has led to its interpretation as a giant quadrupole resonance (GQR). In the lighter nuclei the spectra exhibit a structure similar in character to that observed in the GDR, i.e. there is a series of peaks spread over a broad range of energies. In this work we present results which are typical for light nuclei. The  $^{16}\text{O}$  nucleus is a key one in nuclear structure studies and is the most thoroughly investigated in capture and photo-nuclear reactions. Much work, both theoretical<sup>2</sup> and experimental,<sup>3</sup> has been devoted to the contention that a sizable E2 strength in the continuum region is required to account for the photonuclear data. Wang and Shakin<sup>2</sup> proposed large E2 amplitudes to explain the  $(\gamma, n_0)$  excitation curve, angular distributions and polarization. They suggest that at the lower side of the GDR the E1 and E2 amplitudes are of comparable size. Recent polarized proton capture studies<sup>3</sup> imply that 30% of the Gell-Mann Telegdi<sup>6</sup> E2 sum is located in a broad peak at about 24.5 Mev.

In the present experiment inelastic scattering of 71 Mev  $^3\text{He}$  particles is used to probe the E2 strength in  $^{16}\text{O}$ . The

ABSTRACT

Inelastic scattering of 71 Mev  $^3\text{He}$ -particles from  $^{16}\text{O}$  shows an enhancement and structure of the continuum consistent with the assumption of a giant quadrupole resonance. Completely microscopic model calculations indicate that the excitation of  $1^-(T=1)$  and  $0^+(T=0)$  states may account for only ~10% of the total cross sections of the excitation region 17-27 Mev.

NUCLEAR REACTION  $^{16}\text{O}(^3\text{He}, ^3\text{He}'), E_x = 0-35$  Mev  
 $E_{^3\text{He}} = 71$  Mev; measured  $\sigma(E_x, \theta)$ , deduced E2 strength.

<sup>†</sup>Supported by the National Science Foundation.

results are in agreement with the present picture of  $^{16}\text{O}$  which shows a substantial E2 strength spread over a broad region of excitation energy.

#### EXPERIMENT

71 MeV  $^3\text{He}$ -particles were produced by the Michigan State University Cyclotron. The scattered particles were detected and identified in a silicon counter telescope arranged in the manner suggested by Garvey, *et al.*<sup>7</sup> to minimize slit scattering. The 0.2 mm  $\Delta E$  and 3mm E detectors were placed 5 cm apart and the collimator was located half way between them. The energy resolution was 120 keV, limited primarily by the kinematic spread and target energy loss effects. The target was a 15 cm diameter gas cell filled to 200 torr with oxygen. Beam currents were limited to 300 nA to prevent punctures of the 0.013 mm Kapton windows on the gas target.

Fig. 1 shows a spectrum from the  $^{16}\text{O}(^3\text{He}, ^3\text{He})^{16}\text{O}$  reaction. The data were taken at lab angles between  $10^\circ$  and  $30^\circ$ . Excitation energies shown in the figure are accurate to 30 keV and were determined from an energy calibration based on known states in  $^{16}\text{O}$ , including energy loss corrections for the gas target. The  $^{16}\text{O}$  data are compressed into 150 keV wide channels and replotted in Fig. 2 to show the resemblance to the spectra observed in heavier nuclei. There is a broad enhancement in the excitation energy region 17-27 MeV in  $^{16}\text{O}$  as well as many resolved peaks. Rather narrow states are observed at 17.2, 17.8, 18.5, 19.1 and 20.0 MeV.

Angular distributions were extracted for the low lying states as well as for various components of the continuum. The latter consists of many resolved and unresolved states in the region 17 to 27 MeV on top of a background whose shape is not known. This background is due in part to direct excitation of nuclear states that may give rise to a flat yield, and in part to three body (or more) processes. We have assumed a linear background as shown in Fig. 1. The shaded area reflects the uncertainties in subtracting the background and amounts to 30% of the extracted yield in the 17-27 MeV region. The angular distribution for some low lying states and for the 17-27 MeV region are shown in Figs. 3 and 4.

#### DWBA ANALYSIS

Distorted Wave Born Approximation (DWBA) calculations for T=0 excitations were performed using phenomenological collective models. The differential cross-sections for the monopole breathing mode (MBM) and the T=1 GDR were also calculated using a microscopic description of the excitation mechanism involved.

The prescription for the collective (MBM) radial form factor is taken to be that given by Satchler<sup>8</sup>

$$F(r) = -XU(r) - R \frac{\partial U}{\partial r} \quad (1)$$

where  $U(r)$  is the usual complex optical potential and  $X$  is a constant determined by volume conservation and is about 2.5.



The second term in expression (1) is the conventional surface peaked collective form factor. Only the second term was used in calculating the isoscalar excitations. Expression (1) suggests that the monopole cross-section is very sensitive to the interference between the volume and surface term. A DWBA estimate for a T=1 dipole excitation can also be made using a collective model approach,<sup>9</sup> provided one knows the asymmetry potential for the incident  $^3\text{He}$  particles. In general very little is known about the  $\frac{N-Z}{A}$  term of the  $^3\text{He}$  optical potential but, of course, for N=Z nuclei one expects the coupling interaction to vanish.

The GDR and the MBM cross-sections were therefore estimated using completely microscopic descriptions of these excitations. This procedure has been shown to work well for many different multipole excitations in  $^{40}\text{Ca}$ .<sup>10</sup> In these cases the form factors,  $F_{\text{LSJT}}(r)$ , are given as<sup>11</sup>

$$F_{\text{LSJT}}(r) = \int_0^\infty V_L(r, r') \rho_{\text{tr}}^{\text{LSJT}}(r) r'^2 dr' \dots \quad (2)$$

where L, S, J and T label the orbital, spin, total angular momentum and isospin transferred,  $V_L(r, r')$  is the  $L^{\text{th}}$  multipole of the projectile-target nuclear interaction and  $\rho_{\text{tr}}^{\text{LSJT}}(r)$  is the transition density to be calculated from the initial  $-|0^+\rangle$  and final  $|J^\pi\rangle$  nuclear states:

$$\rho_{\text{tr}}^{\text{LSJT}}(r) = \int_0^\infty \rho_p(r-r') \langle J^\pi || \int_1 \frac{\delta(r'-r_1)}{r_1^2} T_{\text{LSJT}}(\hat{r}_1) || 0^+\rangle d^3r' \quad (3)$$

Here  $\rho_p$  denotes the charge distribution of the proton and i refers to target protons and target neutrons.  $T_{\text{LSJT}}$  is a

spherical harmonic for S=0 and a spin angle tensor for S=1. All nuclear information is contained in the reduced matrix element which is often called the point transition density.

The wave functions employed in this work for the GDR were calculated by T.T. Kuo<sup>12</sup> in the random phase approximation (RPA). Similar results were obtained using the wave functions of Gillet and Vinh-Mau.<sup>13</sup> For the MBM we used the wave functions of Vinh-Mau and Brown.<sup>14</sup> The model space for the GDR includes all lp-lh excitation of  $1h\omega$  and for the MBM all lp-lh and 2p-1h excitations of  $2h\omega$ . Five dipole states are predicted in the 13-26 MeV region of which only the two states at 24.9 and 25 MeV make significant contributions to the dipole cross-section. The monopole strength is mostly concentrated in one state at 21.7 MeV. We note that the effect of the many other complicated configurations in this region should be mainly on the spreading width and the detailed strength distribution. In particular the position of the monopole states might be very sensitive to the degree of sophistication of the model space. Nevertheless we do not expect these complicated configurations to alter significantly the total strength calculated with the simple wave functions mentioned above. Thus the lp-lh model should be suitable for an estimate of the GDR and MBM cross-sections in the region of 17-27 MeV.

The projectile-target nucleon force is taken to be that given by Satchler<sup>15</sup>

$$V_{\text{ST}}(r) = V_{\text{ST}} e^{-\gamma|r-r'|} \quad \dots \quad (4)$$

where

$$V_{00} = -22.5 \text{ MeV}, V_{01} = V_{10} = V_{11} = 2.5 \text{ MeV and } \gamma = 0.20 \text{ fm}^{-1}$$

(This interaction was obtained by folding a two nucleon interaction of Gaussian shape with a Gaussian form representing the projectile size to obtain an effective projectile-target nucleon interaction). The densities in expression (3) were calculated using harmonic oscillator radial wave functions (oscillator parameter  $\alpha = 0.498$ ).

The predicted angular distributions for some of the low lying states and for various other multipoles are displayed in Figs. 3-5. The curves in Fig. 5 for  $L \geq 2$  are normalized to exhaust the Energy Weighted Sum Rule  $1^7$  (EWSR) for  $E_x = 20 \text{ MeV}$ . The curves for the monopole and dipole states are the microscopic calculation results. Their magnitude is absolute in the sense that it emerges from the wave functions and two body interactions which are used. Angular distributions for some low lying states are given in Fig. 3. The curves for the  $3^-$  level at 6.13 MeV and the  $2^+_{-1}$  doublet at  $\sim 7 \text{ MeV}$  were normalized using deformation parameters obtained in other inelastic scattering experiments.<sup>18</sup> A pure  $L=2$  curve (the dashed curve) is shown for comparison.

In Fig. 3 we also show the angular distribution for the  $2^+$  state at 11.52 MeV. The  $2^+$ , 6.92 MeV and the 11.5 MeV states together exhaust

about 20% of the energy weighted quadrupole sum (EQQS). States observed in high energy electron scattering<sup>19</sup> at 11.0 and 12.0 MeV were suggested to be  $2^+$  states also, but more recent data<sup>20</sup> does not confirm these assignments. If the states observed at 11.09 MeV and 12.04 MeV in the present work were  $2^+$  states, then the fraction of the EQQS exhausted would be increased by about 5%. Other small contributions may come from the levels at 9.85, 13.0, 15.2 and 16.5 MeV. Thus the bulk of the E2 strength is expected to be located above 17 MeV in excitation. Other evidence for  $2^+$  states in the region 17-27 MeV will be discussed in the following section. The angular distributions for this region is given in Fig. 4. An  $L=2$  shape is preferred although an  $L=3$  shape cannot be ruled out because of the large uncertainties attached to the experimental points. A large contribution from higher  $L$  can be ruled out. The solid curve shown in Fig. 4 represents the sum of 75% of the EQQS and the  $J^\pi = 1^-$  ( $T=1$ ) cross-section (dashed curve) estimated using detailed wave functions. Note that the total contribution from the dipole-states is small. Also the monopole strength is very weak as can be seen in Fig. 5, and therefore cannot provide an explanation for the enhancement of the continuum. We also show in Fig. 4 the experimental angular distribution of the 8.87 MeV  $2^-$  state which is markedly different from that of the gross structure.



## DISCUSSION

There are a number of known  $2^+$  states in  $^{16}\text{O}$  below 20 MeV excitation energy, and there is also some evidence for  $2^+$  strength at higher energies from  $(\gamma, n)$ ,  $^2(\alpha, \gamma)$  and  $(p, \gamma)$  studies.<sup>3</sup> The results from the present experiment are in reasonable agreement with these previous measurements. States are observed at 9.84, 11.52, 13.11, 16.46, 17.19 and 19.09 MeV which match fairly closely some of the known  $2^+$  states in  $^{16}\text{O}$  (see Table I). As mentioned above, the cross sections for the 6.92 MeV and 11.5 MeV states exhaust about 20% of the EWQS. The  $2^+$  states at 9.85 and 13.1 MeV represent a much smaller fraction of that sum rule.

At higher excitation energies, the information on  $2^+$  states is more sparse. Snover *et al.*<sup>5</sup> found  $2^+$  states at 13.2, 15.9 MeV, 16.5 MeV, 18.3 MeV, 20.0 MeV and 26.5 MeV in a recent  $^{12}\text{C}(\alpha, \gamma)$  experiment. These states, presumably of  $T=0$  character, exhausted about 17% of the EWQS. A  $^{15}\text{N}(p, \gamma)$  capture experiment with polarized protons<sup>3</sup> found about 30% of the quadrupole strength between 20 and 27 MeV of excitation, but the strength was distributed over the whole excitation energy region. Wang and Shakin<sup>2</sup> on the other hand, in fitting photoneutron cross sections and polarizations, assumed that the E2 sum rule was exhausted by a state at 22.5 MeV excitation with a width of 10 MeV. This is much more strength than was found either by the  $^{15}\text{N}(p, \gamma)$  or  $^{12}\text{C}(\alpha, \gamma)$  measurements. Of course the capture measurements are only able

to measure the strength present in the ground state channel; the remaining strength may be present in other channels.

As shown in Fig. 4, the inelastic  $^3\text{He}$  cross section for the region 17-27 MeV matches fairly well an  $L=2$  shape and is consistent with about 75% of the EWQS being in this region. Inspection of the spectra shown in Figs. 1 and 2 reveals that the proposed quadrupole strength is approximately equally divided between the regions 17-20 MeV and 20-27 MeV, and the remaining strength lies below 17 MeV in excitation. The spreading of the E2 strength over a wide range of excitation is consistent with the results obtained in photoneuclear and capture reactions.

One question that is raised by the present data concerns the isospin of the E2 strength. Hanna *et al.*<sup>3</sup> assumed that the E2 strength they observed in the GDR region was of  $T=1$  character. The  $L=2$  strength observed in the present experiment is expected to be predominantly isoscalar. The excitation of  $T=1$  states should be weaker in inelastic  $^3\text{He}$  scattering since the isospin dependent term of the projectile target interaction is about 3 times smaller than the isospin independent part (see Eq. 4). The  $^3\text{He}$  inelastic scattering cross section is therefore approximately nine times weaker for a  $T=1$  than for a  $T=0$  excitation. The large value of the cross section for the continuum region indicates, therefore, that a large fraction of the E2 strength is of  $T=0$  character.

Applying a response function technique with Skyrme forces, Bertsch and Tsai<sup>22</sup> have calculated the strength distribution and inelastic scattering cross sections for various multipoles.

The  $T=0$  quadrupole strength in  $^{16}O$  is predicted to lie at 20 MeV in excitation while the  $T=1$  quadrupole strength occurs at 37 MeV. Only 15% of the  $T=1$  EWQS is predicted to lie below 32 MeV. Inelastic scattering of high energy  $\alpha$ -particles should shed some further light on the isospin of these excitations.

## ACKNOWLEDGEMENTS

We would like to thank L. Robinson for help during the data acquisition and at some stages of the analysis.

## REFERENCES

1. A. Moalem, W. Benenson and G.M. Crawley, Phys. Rev. Letters 31 (1973) 482.
2. W.L. Wang and C.M. Shakin, Phys. Rev. Letters 30 (1973) 301.
3. S.S. Hanna, H.F. Glavish, R. Avida, J.R. Galarco, E. Kuhlmann and R. LaCanna, Phys. Rev. Letters 32 (1974) 114.
4. R.J.J. Stewart, R.C. Morrison, and D.E. Frederick, Phys. Rev. Letters 23 (1969) 323.
5. K.A. Snover, E.G. Adelberger and D.R. Brown, Phys. Rev. Letters 32 (1974) 1061.
6. M.Gell-Mann and V.L. Telegdi, Phys. Rev. 91 (1953) 169.
7. G.T. Garvey, R. Haight and R.P. Lynch, Nucl. Instr. Meth. 59 (1968) 357.
8. G.R. Satchler, Particles and Nuclei 5 (1973) 105.
9. G.R. Satchler, Nucl. Phys. A195 (1972) 1.
10. G.R. Hammerstein, H. McManus, A. Moalem and T.T.S. Kuo, Phys. Letters 49B (1974) 235.
11. G.R. Hammerstein, R.H. Howell, and F. Petrovich, Nucl. Phys. A213 (1973) 45.
12. T.T.S. Kuo, private communications from S.F. Tsai.
13. V. Gillet and N. Vinh-Mau, Nucl. Phys. 54 (1964) 321.
14. N. Vinh-Mau and G.E. Brown, Phys. Letters 1 (1962) 36.



15. G.R. Satchler, Particles and Nuclei 1 (1971) 233.  
 16. C.B. Fulmer and J.C. Hafele, Phys. Rev. C7 (1972) 631; and C.B. Fulmer, private communication from R.R. Doering.  
 17. A.M. Lane, Nuclear Theory (Benjamin, New York, 1965), p. 79.  
 18. D. Bayer, Ph.D. Thesis, Michigan State University, 1970, (unpublished).  
 19. G.J. Vanpraet and W.C. Barber, Nucl. Phys. 79 (1966) 550.  
 20. M. Stroetzel, Phys. Letters 26B (1968) 376.  
 21. F. Ajzenberg-Selove, Nucl. Phys. A166 (1973) 1.  
 22. G.F. Bertsch and S.F. Tsai, to be published.

TABLE I.--2<sup>+</sup> States in <sup>16</sup>O.

T	$\Gamma$ (keV)	Compilation <sup>a</sup> $E_x$ (MeV)	(e,e') <sup>b</sup> $E_x$ (MeV)	( $\alpha,\gamma$ ) <sup>c</sup> $E_x$ (MeV)	(He, <sup>3</sup> He) <sup>3',d</sup> $E_x$ (MeV)
0		6.919	6.92		6.92 <sup>e</sup>
	1.1	9.847	9.85		9.84
	74	11.521	(11.0)		
	150	13.02	11.52		11.52
	250	13.14	(12.0)		
(0)	660	15.26	13.0	13.2	13.11
	45	16.407	15.15		
	280	16.94	16.48		16.46
		(17.10)			
	200	17.17			17.2
	30	(17.755)			17.8
	390	18.18		18.3	18.5
	260	(18.71)			
1	120	19.06			19.1
	41	(19.12)			
(1)	120	(19.90)			
2	50	24.52	24.52	20.0	20.0
				26.5	

<sup>a</sup>Ref. 21.<sup>b</sup>Ref. 19.20<sup>c</sup>Ref. 5<sup>d</sup>Present experiment<sup>e</sup>Not resolved from 7.12 MeV state.

## FIGURE CAPTIONS

Fig. 1--Energy spectrum from  $^{16}\text{O}(^3\text{He}, ^3\text{He}')^{16}\text{O}$ . The excitation energies shown were determined in this experiment. The positions of known  $2^+$  states are indicated by solid bars. The shaded area indicates the background shape and error in background subtraction.

Fig. 2--Energy spectra from  $^{16}\text{O}(^3\text{He}, ^3\text{He}')^{16}\text{O}$  in 150 keV energy bins.

Fig. 3--Angular distributions for  $^{16}\text{O}(^3\text{He}, ^3\text{He}')^{16}\text{O}$  leading to low lying states. The curves are DWBA predictions. The optical potential includes real and imaginary volume Woods-Saxon shape;  $V=-125.95$ ,  $r=1.05$ ,  $a=0.887$ ,  $W=-17.15$ ,  $r'=1.66$ ,  $a'=0.745$ . These parameters were obtained from a 6 parameters search on elastic scattering  $^{16}\text{O}$  of  $^3\text{He}$  from  $^{27}\text{Al}$ .

Fig. 4--Angular distribution for the excitation energy region 17-27 MeV. The solid curve is the DWBA prediction for the total cross-section of a  $T=0$  quadrupole state which exhaust 75% of the EWS and all  $T=1$  dipole states predicted in this region. The contribution from the dipole state is shown separately as a dashed line. The experimental angular distribution for the  $2^-$  state at 8.87 MeV is also shown at the bottom of the figure. For details of the calculations see text and caption for Fig. 3.

Fig. 5--Differential cross-sections for multipole states in  $^{16}\text{O}$ . The curves for the  $L \geq 2$  are the macroscopic model predictions normalized to exhaust the sum rule limit at  $E_x=20$  MeV. The monopole and dipole cross-section are the microscopic model results: their absolute magnitude is determined by the projectile-target nucleon interaction and the detailed wave functions of the states involved.



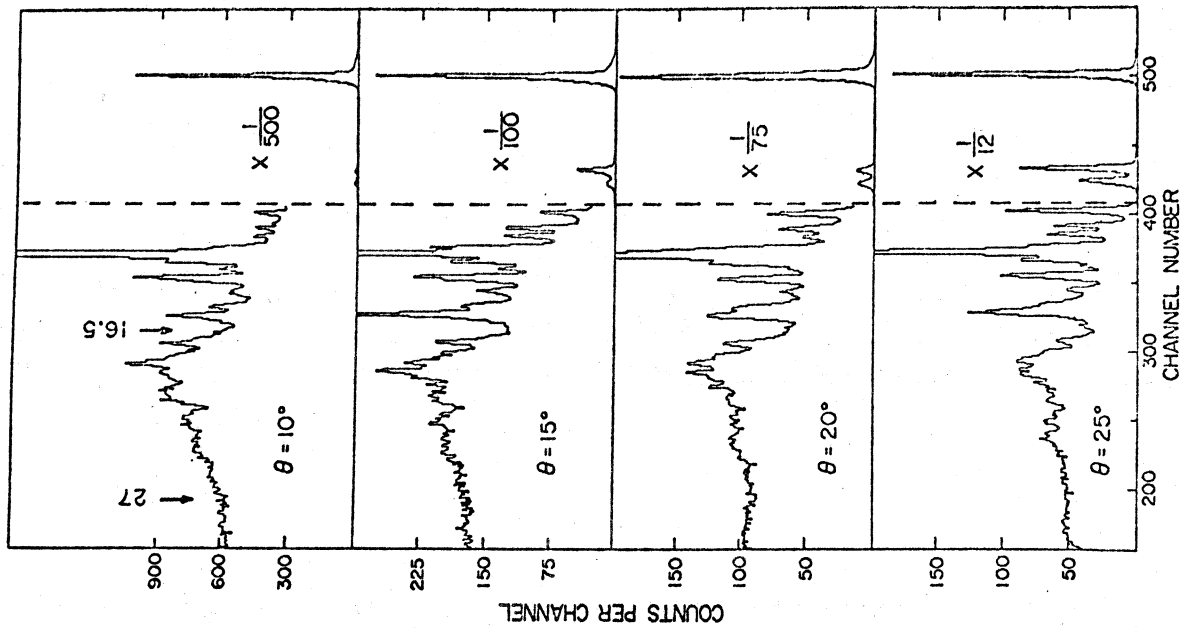


Figure 2

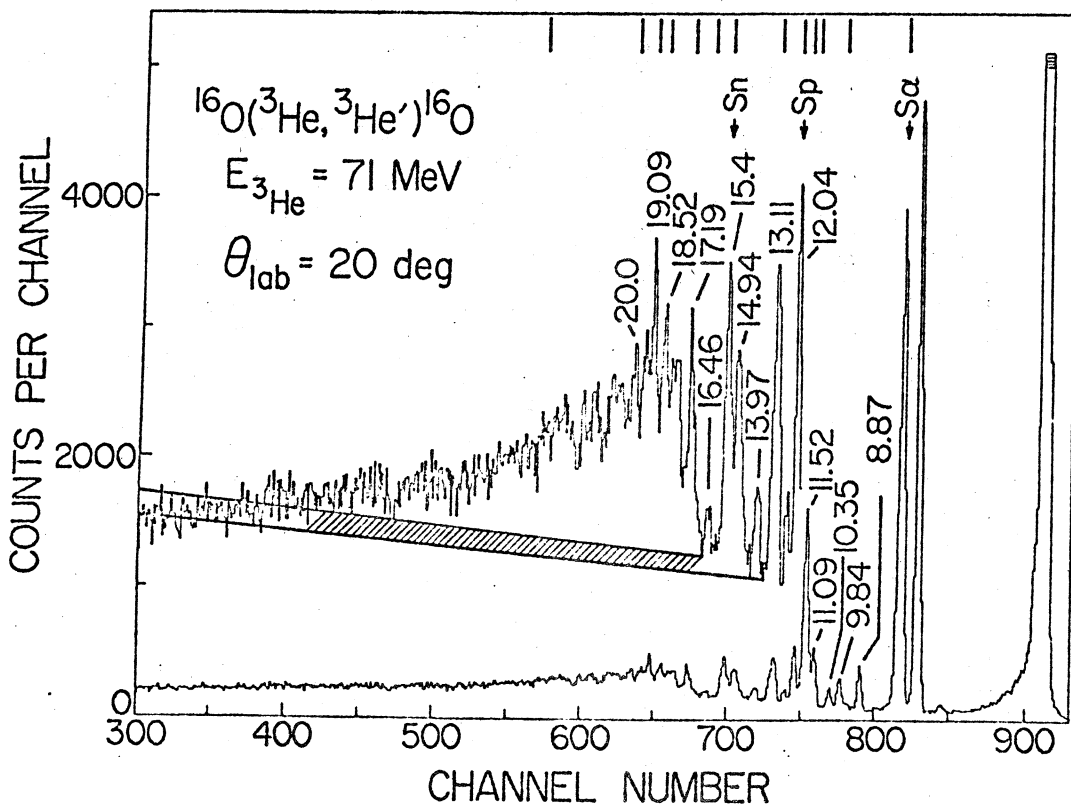


Figure 1

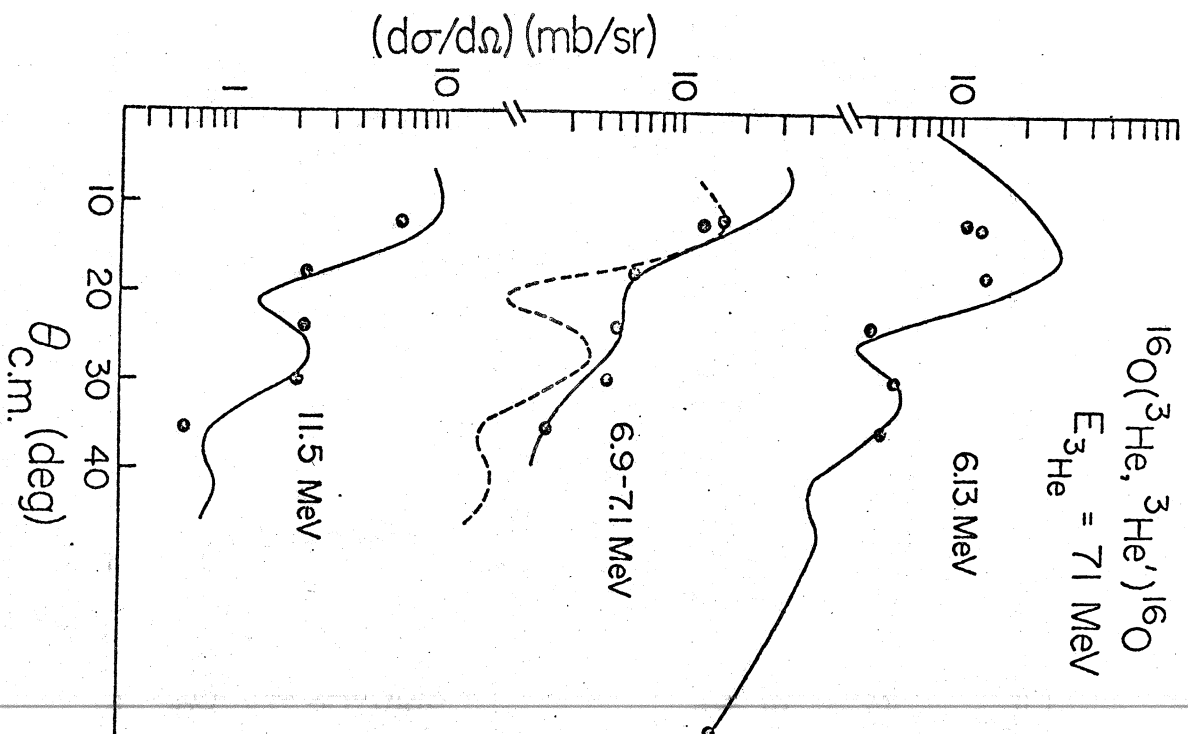


Figure 3

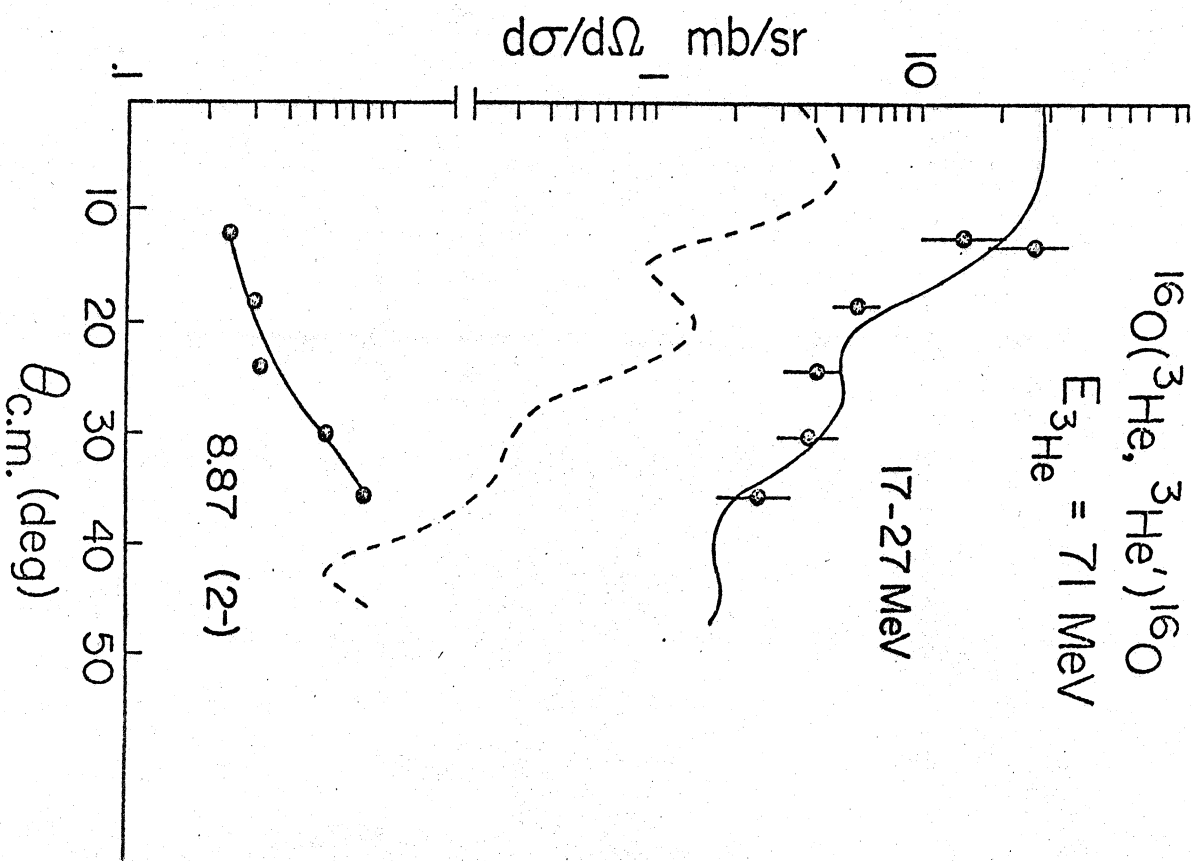


Figure 4



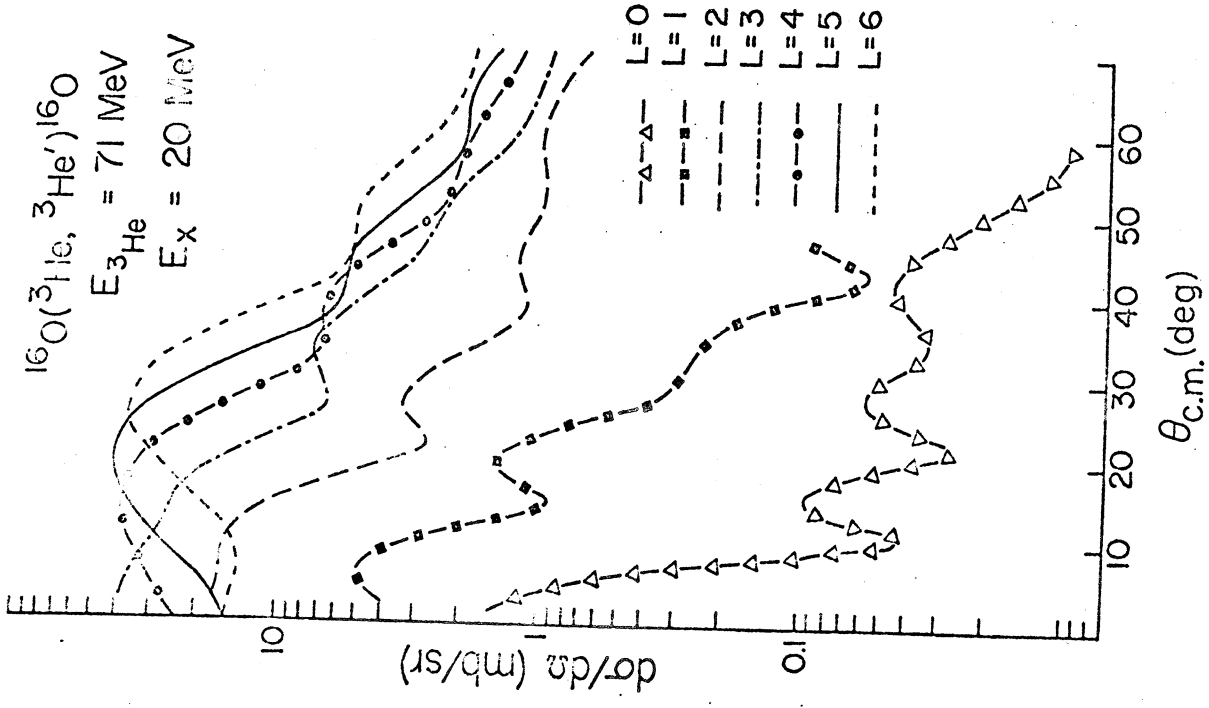


Figure 5

